Int. J. Electrochem. Sci., 15 **(2020)** 10936 – 10954, doi: 10.20964/2020.11.63

International Journal of
ELECTROCHEMICAL
SCIENCE
www.electrochemsci.org

Review

Design Strategies for Enhancing the Electrochemical Performance of Li-Rich Cathode Materials for Lithium-Ion Batteries

Chen Hu[1,†], *Yi Jin*[1,†], *Tianfeng Geng*[2,†], *Dandan Sun*[2], *Chunyu Du*[2,*], *Jiyuan Jian*[2], *Geping Yin*[2]

[1] State Key Laboratory of Operation and Control of Renewable Energy & Storage Systems, China Electric Power Research Institute, Beijing 100192, China
[2] MIIT Key Laboratory of Critical Materials Technology for New Energy Conversion and Storage, School of Chemistry and Chemical Engineering, Harbin Institute of Technology, Harbin 150001, China
† These authors contributed equally.
[*]E-mail: cydu@hit.edu.cn

Received: 8 April 2020 / *Accepted:* 27 August 2020 / *Published:* 30 September 2020

Lithium-ion batteries (LIBs) are one of the most promising energy storage technologies for many applications, such as environmentally friendly transportation. The cathode is the most important material in LIBs and determines mainly their energy density, life and cost. Li-rich layered oxides $xLi_2MnO_3·(1-x)LiMO_2$ (M=Mn, Ni, Co) have been recognized as the most attractive candidates for next-generation cathode materials due to their extremely high reversible capacity. However, severe technical issues (mainly, the low initial Coulomb efficiency, poor rate capability, and voltage decay during cycling) need to be addressed. In this review, we summarize recent research progress on Li-rich layered oxide cathode materials. We focus on new strategies for tackling the technical challenges of Li-rich layered oxide cathode materials, which include exposing preferential crystal planes, inducing oxygen/lithium defects, forming spinel-layered or olivine-layered heterogeneous structures and tuning the lattice structure. Future research directions for Li-rich cathode materials are finally proposed for commercial applications.

Keywords: Lithium-ion batteries, Cathode materials, Li-rich layered oxides, Heterogeneous structures, Cycling stability

1. INTRODUCTION

With the rapid development of electric vehicles and energy storage devices, the demand for Li-ion batteries (LIBs) with high energy density and high power density has largely increased[1]. The energy density, long-term cycling stability and safety of LIBs are mainly determined by the electrochemical performance of the electrode materials, particularly the cathode materials[2]. Conventional cathode materials such as $LiCoO_2$, spinel oxides ($LiMn_2O_4$), olivine phosphates ($LiFePO_4$), and layered oxides ($LiMO_2$ (M=Mn, Ni, Co, etc.)) have attracted much attention[3, 4]. However, a low capacity density cannot satisfy the requirements of electric vehicles (EVs) and hybrid electric vehicles (HEVs), which have longer driving ranges[5]. Li-rich layered oxide (LLO) cathode materials, either as a solid solution or as a composite of layered Li_2MnO_3 and $LiMO_2$ (M=Mn, Co, Ni, etc.), not only show superior reversible capacities exceeding 250 mAh g^{-1} but also offer the advantages of low cost, stability and safety. Therefore, Li-rich oxide cathode materials are regarded as the most promising cathode materials for next-generation high energy-density LIBs[6-9].

The intrinsic structure of LLO materials consists of layered $LiMO_2$ ($R\bar{3}m$) and Li_2MnO_3 ($C2/m$), as shown in Fig. 1a. The monoclinic Li_2MnO_3 structure can be considered a particular case of $LiMO_2$ with an M layer consisting of an aperiodic sequence of one Li and two Mn atoms. Therefore, both of these structures can be indexed by layered α-$NaFeO_2$-type rock salt structures, where all the octahedral sites of their closely packed oxygen arrays are occupied. For example, in the XRD pattern (Fig. 1b) of $0.5Li_2MnO_3 \cdot 0.5LiNi_{0.5}Mn_{0.5}O_2$, most peaks can be indexed to a single phase of α-$NaFeO_2$ with a space group of $R\bar{3}m$, while the splitting peaks of (018) and (110) and of (006) and (012) are thought to be evidence for the degree of ordering of the layered structure. Furthermore, the wide and slight peaks from 20°-25°are attribute to the monoclinic super-lattice structures of $LiMn_6$.

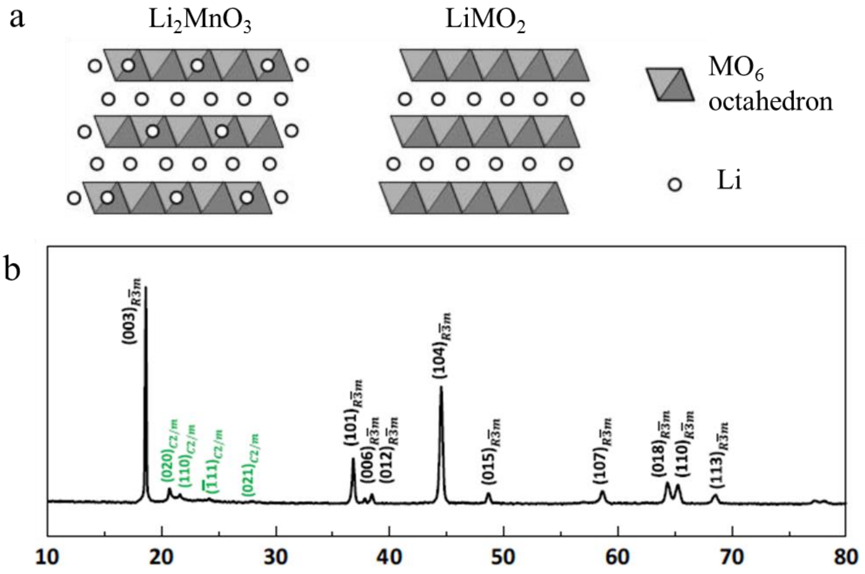

Figure 1. The crystal structure of LLO materials. (a) Li_2MnO_3 (space group: $R\bar{3}m$) and $LiMO_2$ (space group: $C2/m$). Reprinted with permission from The Royal Society of Chemistry. (b) XRD pattern of $0.5Li_2MnO_3 \cdot 0.5LiNi_{0.5}Mn_{0.5}O_2$. Reprinted with permission from the Electrochemical Society[6].

To understand the charge-discharge process associated with the complicated electrochemical reaction mechanism, a classic two-dimensional phase diagram (Fig. 2) is used to show the electrochemical reaction pathways of LLOs[6]. During the initial charge process, when the voltage is charged to approximately 4.4 V, Li is extracted from the $LiMO_2$ component with a simultaneous oxidation of M^{3+} to M^{4+}. When the voltage is up to approximately 4.5 V[6, 10-12], 2Li are extracted from the Li_2MnO_3 component[13, 14], accompanied by the irreversible loss of oxygen to compensate for the diffusion of lithium to tetrahedral sites in the lithium-depleted layer, thereby providing additional capacity to maintain the structural stability. This mechanism has been confirmed by scientists using MAS, NMR[15] and theoretical calculations[16]. However, only 1Li can be reinserted into the Li layer, resulting in an inferior initial Coulombic efficiency. At the same time, the oxidation of oxygen causes partial oxygen evolution accompanied by structural rearrangement, which leads to a gradual change from the layer structure to the spinel-like or rock-salt structure in the redox reactions, along with cycling[17-19].

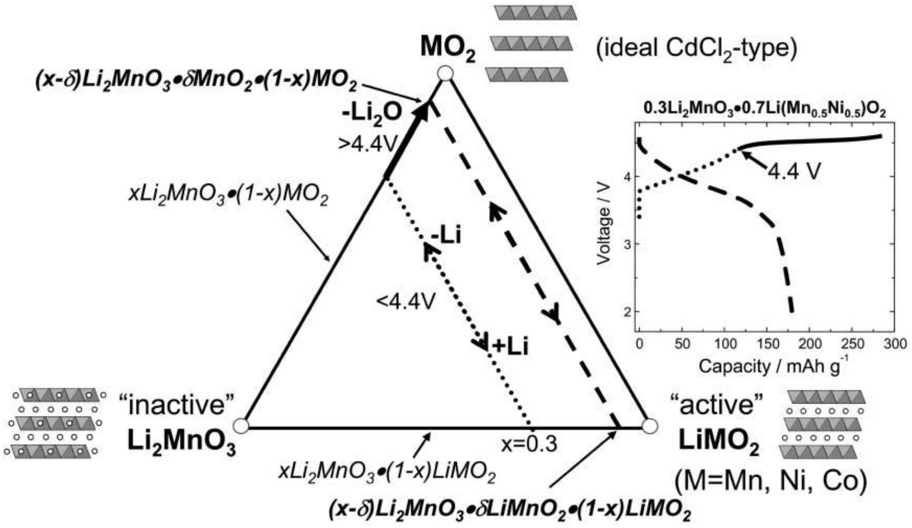

Figure 2. Compositional phase diagram showing the electrochemical reaction pathways for a $xLi_2MnO_3\cdot(1-2x)LiMO_2$ electrode. Reprinted with permission from The Royal Society of Chemistry[6].

Recent investigations on the electrochemical mechanism have revealed that anion redox might supply additional capacity[20-22]. Pearce et al.[23] found that during the charge process of Li_2IrO_3, there are some co-existing reversible cationic and anionic redox reactions. Simultaneously, this phenomenon was visually observed by transmission electron microscopy (TEM) neutron diffraction and X-ray photoelectron spectroscopy (XPS) experiments, which were consistent with the theoretical calculation. This discovery opened up a new means for exploring the reaction mechanism of LLO cathode materials.

However, LLO materials still face some obstacles for the real commercial application of LIBs: (1) the Li_2MnO_3 component in the $xLi_2MnO_3\cdot(1-x)LiMO_2$ (M=Mn, Ni, Co, etc.) composite has low ionic/electronic conductivities, resulting in a large charge transfer impedance and thus inferior rate stability; (2) during the charge/discharge process, side reactions between LLO materials and electrolytes at high potentials likely occur, which transform the layer structure to the spinel/rock salt phase, leading to poor cycling performance; (3) the traditional hexagonal layered structure can supply only a 2D Li^+ diffusion plane, reducing the Li^+ transfer efficiency.

Researchers have made great efforts to overcome these obstacles of LLOs, and substantial, promising progress has been made. In this review, we provide a detailed summary of the recent research progress on LLO cathode materials with a focus on the strategies for performance enhancement. The conventional methods, including element doping and surface coating, have been well summarized by some reviews and are introduced briefly in this paper. We pay much more attention to more recent and new efforts to increase the electrochemical properties of LLO cathode materials, mainly the rate capability and cycling performance. These effective strategies include exposing preferential crystal planes, inducing oxygen/lithium defects, forming spinel-layered or olivine-layered heterogeneous structures, and tuning the lattice structure. Some of the strategies have become hot topics and are seeing great progress in improving the structural stability and electrochemical properties of layered Li-rich cathode materials. Finally, future research directions regarding Li-rich cathode materials for LIBs are proposed.

2. ELEMENT DOPING AND SURFACE COATING

Researchers have made great efforts to overcome these challenges of LLOs, such as element doping and surface coating. These efforts have been well summarized by some reviews, and therefore, we will introduce them only briefly. Elemental doping is thought to be a meaningful solution for expanding the Li^+ diffusing channels and decreasing the amount of degradation because the elements doped in the crystal structure of LLO materials play an important role in stabilizing the layered crystal structures[21, 24-26]. A large number of publications reported that this method was feasible[27-38]. For instance, Wang et al.[27] doped large Sn^{4+} into the transition metal layer of $Li_2MnO_3{\cdot}LiMn_{0.5}Ni_{0.5}O_2$ to broaden the Li^+ diffusion channels and enlarge the interplanar spacing of the (003) plane. In addition, the doping elements did not change the pristine layer structure of LLO materials; thus, they will not hinder Li^+ intercalation/de-intercalation and improve the electrochemical performance. Similarly, Li et al.[28] reported that doping ‘super-large’ Y^{3+} could expand the Li^+ diffusion pathway, stabilize the crystal structure and enhance the cycling stability of $Li_{1.2}Mn_{0.6}Ni_{0.2}O_2$.

Building a surface protecting layer is also very meaningful and the most common method for enhancing the electrochemical stability and improve the electronic or ionic conductivity of LLO materials. A certain thickness of the homogeneous coating layer can restrain the side reactions between the electrode and electrolyte, alleviating the metal-Li mixing in the crystal structure of LLO materials. Many compounds coated on the surface of Li-rich cathode materials have been investigated, such as various metal oxides[39-47], fluorides[48-53], phosphates[54-59], active cathode materials and some organic materials[60]. Oh et al.[61] reported a new surface treatment method for the Li-rich cathode material $0.4Li_2MnO_3{\cdot}0.6LiNi_{1/3}Co_{1/3}Mn_{1/3}O_2$, in which a hybrid coating layer is constructed, including a graphene oxide layer and a reduced graphene oxide layer, via hydrazine treatment on the surface of a Li-rich cathode material. The resulting material had a higher electronic conductivity, and the surface treatment stabilized the structure of Li_2MnO_3 and prevented the transition metal migration from the transition metal layer to the Li slab during the cycling process because hydrazine could react with only the Li_2MnO_3 phase of $0.4Li_2MnO_3{\cdot}0.6LiNi_{1/3}Co_{1/3}Mn_{1/3}O_2$. In addition, this surface treating method can form a uniform coating layer and control the thickness of the graphene-oxide-coated material. Therefore, the coated materials had excellent initial Coulombic efficiency (99.5%) (Fig. 3a) and excellent rate performance (Fig. 3b). Liu et al.[62] aimed to reduce the voltage and capacity decay by combining the doping and coating methods for $Li_{1.17}Ni_{0.17}Co_{0.17}Mn_{0.5}O_2$. They doped Mg^{2+} in the bulk Li layer of Li-rich materials because the ion radii of Mg^{2+} and Li^+ are similar. Mg^{2+} could enter the Li site to avoid transition metal migration from the transition metal layer to the Li layer during cycling. Meanwhile, coating $LiMgPO_4$ on the surface of the material suppressed the decomposition of the electrolyte. The hybrid treatment method improved the initial Coulombic efficiency and rate capacity, showing good structure stability and slower voltage deterioration even at high temperatures (Fig. 3c and d).

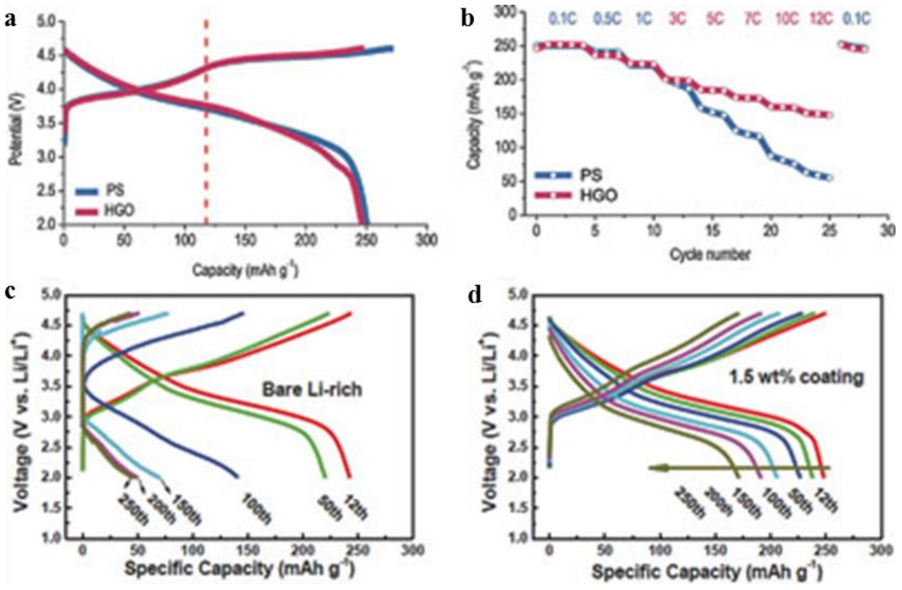

Figure 3. (a) Voltage profiles of PS and HGO cathodes in coin-type half-cells between 2.0 V and 4.6 V with a 0.1 C-rate (=20 mA g^{-1}) at 24 °C. (b) Rate capabilities of coin-type half-cells with C-rates increasing from 0.1 to 12 C between 4.6 V and 2.0 V at 24 °C. (c and d) Charge–discharge profiles of bare and surface-modified Li-rich cathode materials at different cycle numbers. Reprinted with permission from Wiley VCH[62].

3. EXPOSING PREFERENTIAL CRYSTAL PLANES

Despite the encouraging progress, the traditional doping and surface coating methods cannot satisfactorily improve the electrochemical performance of LLO cathode materials, and they cannot meet the stringent requirements of electric-vehicle applications. To address these issues, some more effective approaches must be explored to increase the comprehensive electrochemical properties. The exposure of particular preferential planes could offer a fast intercalation/deintercalation pathway to improve Li^+ transport efficiency and thus attract attention towards LLO cathode materials.

It is very important that Li ions be transported unimpededly in the layered structure of Li-rich cathode materials[63]. The hexagonal layer structure with the *R*3*m* space group is indexed mainly by the (001) plane arranged with a MO_6 (M=Ni, Co, Mn, etc.) octahedron, parallel to the Li^+ layers along the a (or b) axis[64, 65]. However, the closely packed (001) plane hinders Li^+ transport along the c axis, being electrochemically inactive for Li insertion/reinsertion during the charge/discharge process[66, 67]. It was reported that Li-rich LLO materials with an exposed (010) plane on the surface that is perpendicular to the (001) plane could supply a thoroughfare for Li-ion transport (Fig. 4) compared with the other five facets of the hexagonal crystal structure[63, 68, 69]. Nevertheless, the (001) face has lower surface energy; thus, LLOs easily expose the (001) plane on the surface. Designing a Li-rich cathode material to promote growth along the c axis would result in the exposure of (010) facets more easily.

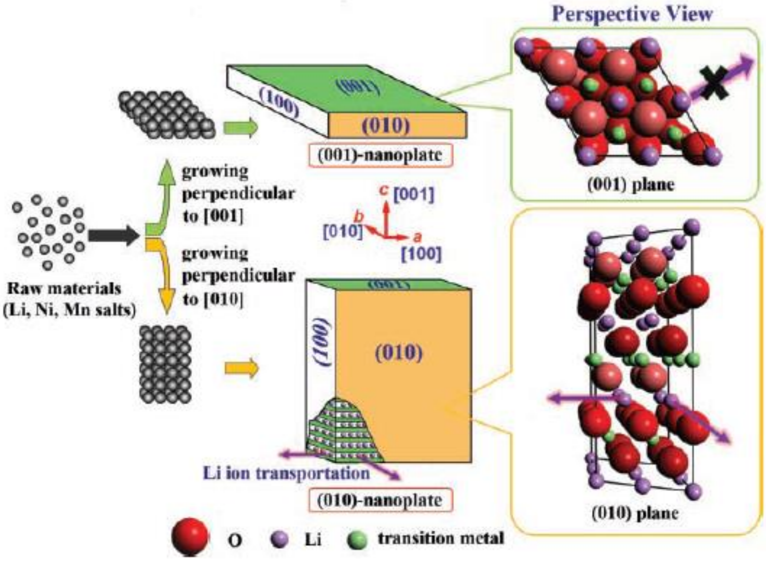

Figure 4. Schematic illustration of two kinds of nanoplates and the microstructure of their surfaces. Reprinted with permission from Wiley VCH[69].

Chen et al.[70] proposed a novel quasi-sphere hierarchical structure of Li-rich materials with $Li_{1.2}Ni_{0.2}Mn_{0.6}O_2$ nanoplates self-assembled during the conventional co-precipitation process, and they confirmed the exposure of the (010) plane on the surface of materials (Fig. 5b) by high-resolution transmission electron microscopy (HRTEM) and selected area electron diffraction (SAED). This three-dimensional network structure could provide excellent ion and electron transport channels for Li^+ insertion/extraction. Therefore, the materials exhibited a superior rate capacity of up to 141.7 mAh g^{-1} at 20 C (1 C=250 mA g^{-1}) and excellent cycling performance (Fig. 5a). However, the high-temperature calcination of chemical lithiation would destroy the nanoplates and cause agglomeration, although high temperature is essential for transition metals to achieve superior crystallinity[68, 71]. Recently, Xu et al.[72] designed LLO nanoplates with (010)-oriented orthogonal arrangements via a hydrothermal method, alleviating the tendency of nanoplates stacking on the high-energy exposed (010) plane surface. At the same time, they found a spinel phase in the Li-rich layered structure by combining XRD and TEM, which supplied Li^+ transport tunnels, improving the Li^+ transport kinetics and stabilizing the crystal structure. Therefore, the materials presented a Coulombic efficiency of 93% and excellent rate stability (Fig. 5c).

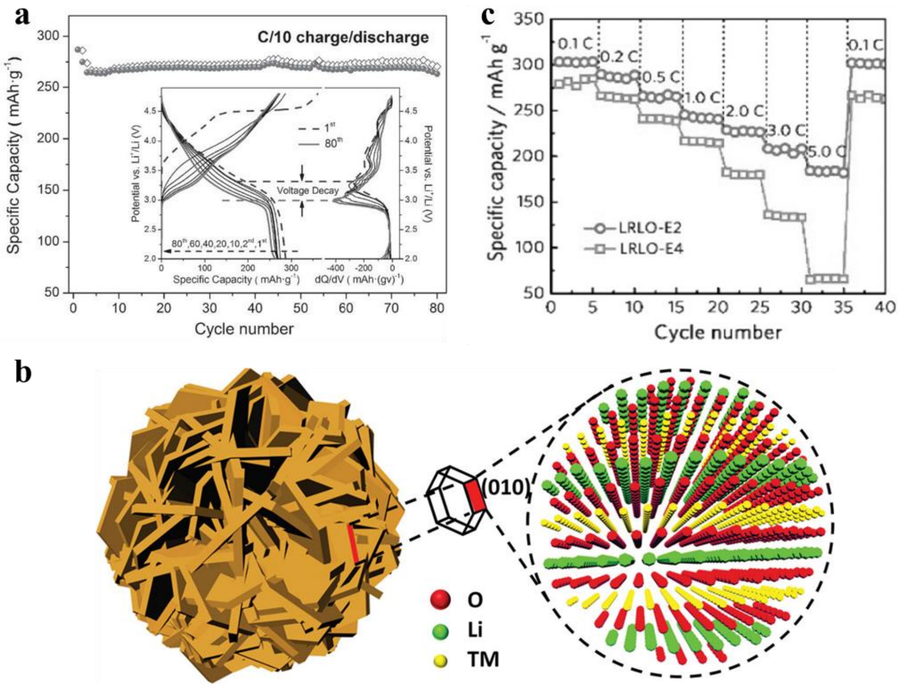

Figure 5. (a) Comparison of the initial charge/discharge curves. Reprinted with permission from The Royal Society of Chemistry. (b) Schematic illustration of hierarchical-structure lithium-rich material. Reprinted with permission from Wiley VCH. (c) Rate capability at different rates of LRLO-E2 with the OAN-ST structure and LRLO-E4 with the stacked nanoplate structure. Reprinted with permission from the American Chemical Society[70,71].

4. INDUCING OXYGEN/LITHIUM DEFECTS

Vacancies play an important role in determining the electronic and ionic transfer performances of Li-rich cathode materials[73, 74]. Qiu et al.[75] fabricated oxygen vacancies on the surface of a Li-rich cathode material via a gas-solid interface reaction (Fig. 6), which was achieved by carrying out a gas-solid reaction between Li-rich layered oxides and carbon dioxide to form Li_2CO_3. At the same time, the presence of oxygen vacancies could suppress the generation of O_2 gas, avoiding irreversible Li_2O loss from the structure, which leads to transition metal ion migration and structural phase change at high potentials of the initial charge process, further promoting voltage decay for the subsequent cycling process. In addition, they proposed that the O^{2-}/O^{-} or $O_2{}^{2-}$ reversible redox reaction during Li^+ insertion/reinsertion decreases O_2 gas loss. This modified Li-rich cathode material showed excellent electrochemical performance with an initial discharge capacity of 301 mAh g^{-1} and an initial Coulombic efficiency of up to 93.2% at 25 mA g^{-1}. After 100 cycles at the same current density, the capacity retention was almost 100%, and no obvious voltage decay was observed (Fig. 7a and b). Even at the high temperature of 55 °C, the modified Li-rich cathode material also showed superior structural stability, with a capacity retention of 93.27% after 150 cycles at a 1 C-rate (Fig. 7c).

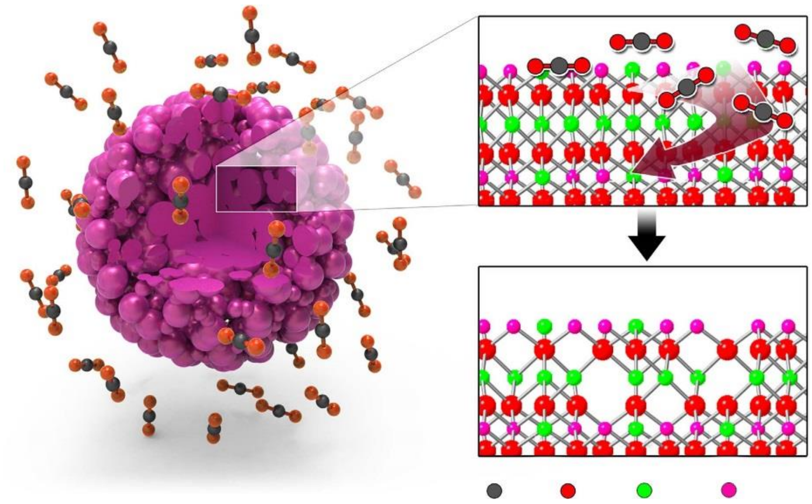

Figure 6. Schematic of GSIR between Li-rich layered oxides and carbon dioxide. Reprinted with permission from Nature[75].

Almost at the same time, Chen et al.[76] reported that nano-SnO_2-coated $Li_{1.2}Mn_{0.54}Ni_{0.13}Co_{0.13}O_2$ would surprisingly improve the cycling performance and rate capacity. This phenomenon was explained by the existing oxygen vacancies in the nano-SnO_2 coating layer, which supplied a fast Li^+ transfer pathway because the high-valence-state oxygen would go through the coating layer and improve the activation of Li_2MnO_3.

In addition to the oxygen vacancies that are profitable for Li-ion transfer in Li-rich cathode materials, reducing the content of Li during the lithiation process, which dominates the Li vacancy, could regulate the Li-rich layered structure. Xu et al.[77] prepared porous carbonate precursors by a hydrothermal method and then incorporated different quantities of LiOH in the process of chemical lithiation. This method generated the hetero-epitaxial layer-spinel structure of LLOs. The materials showed a superior discharge capacity of 307 mAh g^{-1} at 0.1 C and excellent rate stability. They conjectured that at high-temperature calcination, a Li-deficient environment would cause transition metal migration from 3b to 16d octahedron sites, along with Li^+ moving from 3a to 8a tetrahedron sites, producing an epitaxial spinel structure in the layer structure (Fig. 8).

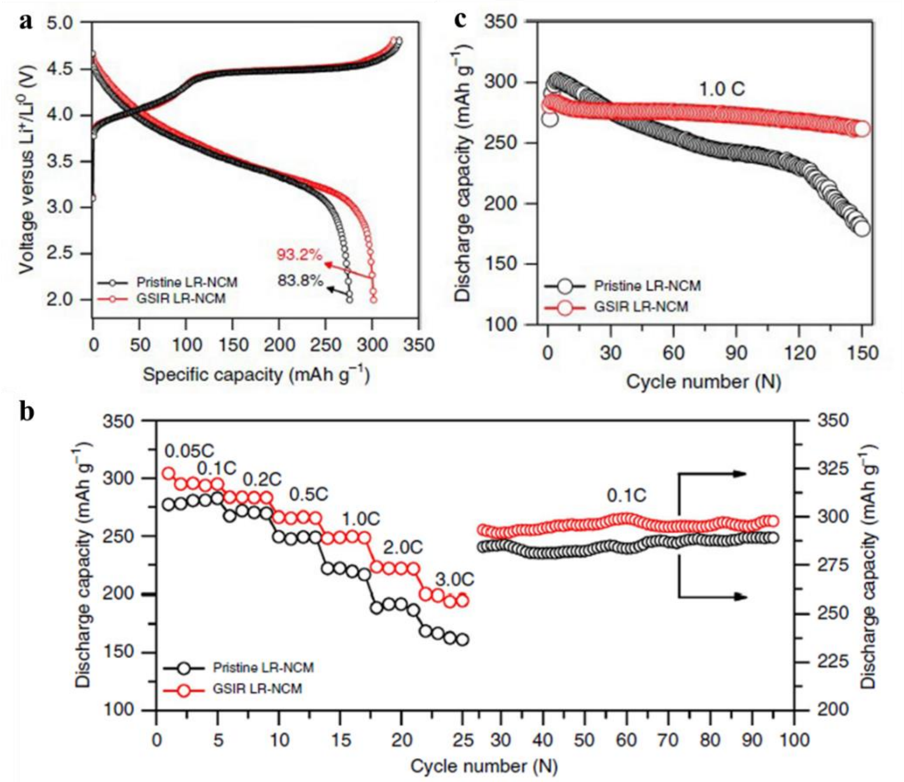

Figure 7. (a) First charge–discharge profiles of pristine and GSIR LR-NCM at a 0.05 C-rate. (b) Discharge-rate capacity after galvanostatic charging at a 0.1 C-rate before each discharge. The capacity retention when performing charge–discharge cycles at a 0.1 C-rate for 70 cycles after all the rate tests is shown. (c) Cycling performance of pristine and GSIR LR-NCM at 55 °C achieved by applying a constant current density with a 1.0 C-rate. Reprinted with permission from Nature[75].

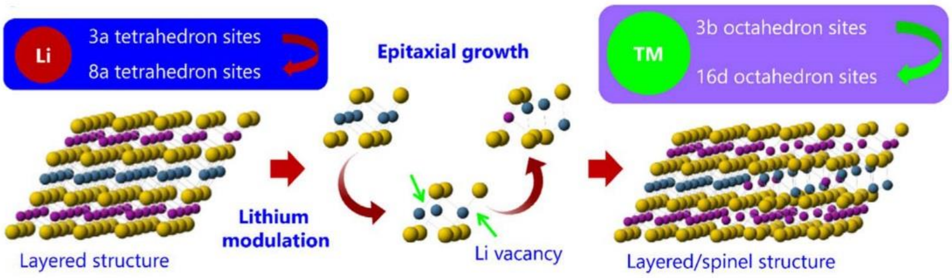

Figure 8. A possible mechanism leading to the hetero-epitaxial nanostructure in the S/LLO composite. Reprinted with permission from Elsevier[77].

5. LAYERED-SPINEL HETEROGENEOUS STRUCTURE

Since the 2D layered structure of Li-rich materials suffers from poor electrochemical performance, a rational architecture design has been considered as an effective avenue for further enhancing their electrochemical performance. Composite cathode materials with different characteristics are always attractive because they can combine the advantages of different components. It is meaningful to controllably synthesize Li-rich cathodes with desirable compositions and hierarchical structures. A number of researchers have constructed hetero-structures for Li-rich cathode materials. Thackeray et al.[78] first proposed the layered-spinel $xLi_2MnO_3·(1\text{-}x)Li_{1+}Mn_{2-□}$□□ composite, which could vary the composition of the layered-spinel composite and the length of the voltage plateau at ~4.5 V during the initial charge. This layered-spinel composite showed a superior specific capacity and cycling performance. Spinel structure cathode materials such as LiM_2O_4 (M=Ni, Co, Mn, etc.) facilitate 3D Li^+ diffusion and offer superior rate performance, which could offset the drawbacks of Li-rich cathode materials[79-82]. Therefore, incorporating spinel Mn-based cathode materials into/on Li-rich layered oxides to construct layered-spinel hetero-structure composites would address the poor rate stability of LLOs and provide surprising capacity and cycling performance even at high voltages[83-85].

Bhaskar et al.[86] incorporated $Li[Ni_{0.5}Mn_{1.5}]O_4$ into $0.6Li_2MnO_3·0.4[LiCo_{0.333}Mn_{0.333}Ni_{0.333}]O_2$ for different stoichiometric ratios, with the aim of presenting the structural characteristics of Li-rich and spinel phases. The physical characterization confirmed that the composite samples were successfully synthesized by combining gravimetric analyses and XRD. At the same time, for different spinel contents, the electrochemical properties appear prodigiously distinctive, although all the composites have a reasonable capacity.

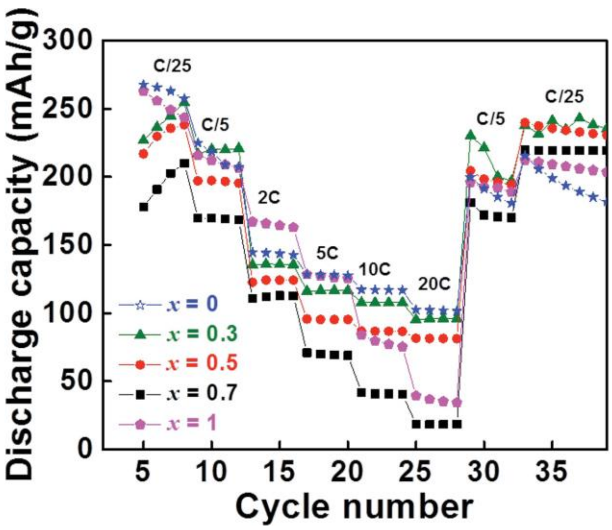

Figure 9. Rate performance of *x* LIR·(1 – *x*)LNMO (*x*=0.0, 0.3, 0.5, 0.7, 0.1). Reprinted with permission from Wiley VCH[86].

Among these materials of $x\{0.6Li_2MnO_3·0.4[LiCo_{0.333}Mn_{0.333}Ni_{0.333}]O_2\}·(1–x)Li[Ni_{0.5}Mn_{1.5}]O_4$, the composites with x=0.5 and 0.7 exhibited superior cycling and rate performances (Fig. 9), which resulted from the increased structural stability and fast Li^+ intercalation/deintercalation pathways. Therefore, they concluded that optimizing the proportion of composite materials was worth further investigation. Analogously, Chen et al.[87] coated spinel $LiNi_{0.5}Mn_{1.5}O_2$ on the surface of a Li-rich cathode material by a facile and low-cost method. This spinel coating layer could prevent the interface side reaction between the electrode and electrolyte and be conductive towards Li-ion fast diffusion. Accordingly, the initial discharge capacity and rate stability were strikingly improved.

The calcination temperature has an important effect on the transformation of the crystal structure and thus the electrochemical performance[88,89]. Luo et al.[90] synthesized $Li_{1.2}Mn_{0.4}Co_{0.4}O_2$ via a solvothermal-precursor method, which introduced the spinel-like phase in the layer structure during the heating treatment process.

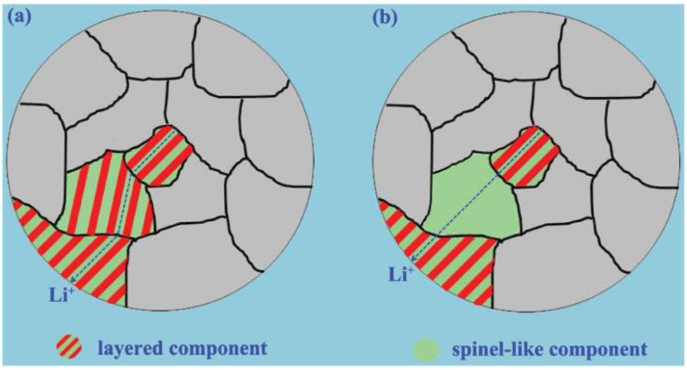

Figure 10. Schematic illustration of Li-ion diffusion within the assembled spheres of the electrode materials (a) T8 and (b) T7 (T7:700 °C for 12 h; T8 800 °C for 12 h). Reprinted with permission from Wiley VCH[90].

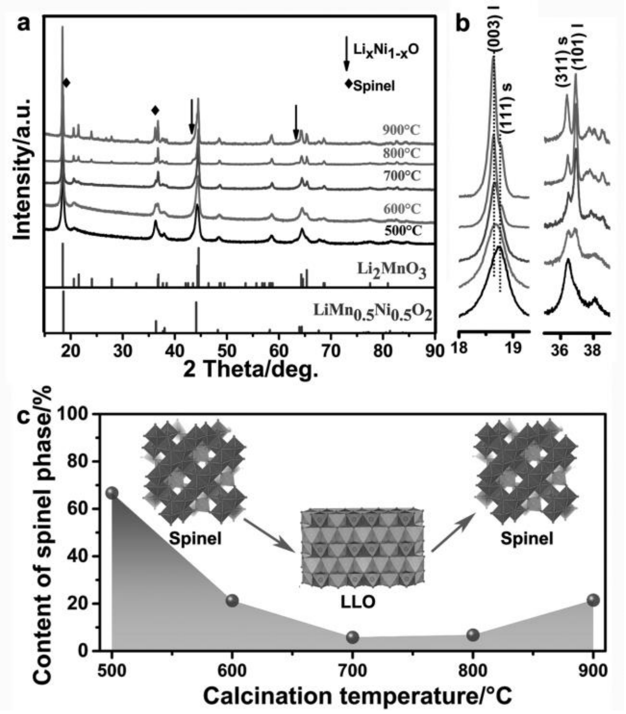

Figure 11. (a) XRD patterns of products calcined at different temperatures in air for 12 h. (b) The amplified region of 18°–19.5° and 35°–39°. (c) Rietveld refinement content of the spinel phase in products calcined at different temperatures in air for 12 h. Reprinted with permission from Wiley VCH[91].

The layered-spinel intergrowth structure was detected when calcined at 700 °C. This 3D structure shortened the transfer pathway of Li^+ in the bulk of the resulting materials (Fig. 10) and reduced the thickness of the solid electrolyte interface layer, leading to a lower charge transfer resistance. Therefore, this layer-spinel material presented a highly improved rate capacity and cycling stability, and its discharge capacity could reach 185.1 mAh g^{-1} even though the current density was 1200 mA g^{-1}. However, the authors did not give a detailed quantitative analysis. Later, Pei et al.[91] synthesized $Li_{1.2}Mn_{0.6}Ni_{0.2}O_2$ by a polyol method with a calcination temperature from 500 °C to 900 °C, which would induce the formation of a spinel phase. They proposed that the electrochemical performance was associated with the content of the spinel phase in layered-spinel-structure cathode materials. Importantly, the ratio of the spinel phase to the layer structure was calculated by XRD Rietveld refinement (Fig. 11). They found that the material showed the best cycling and rate performances at 700 °C because the appropriate content of the spinel phase at this temperature could minimize the influence on the intergranular structure.

Our group has also made some progress in the aspect of forming spinel structures in Li-rich layered materials. We prepared a $Li_{1.2}Ni_{0.13}Co_{0.13}Mn_{0.54}O_2$ material, which further reacted with NH_4HF_2 by a facile solid-phase reaction[92]. This reaction triggered the transformation from a layer to a spinel structure and finally led to the formation of layered-spinel composite materials. This heterogeneous structure, mainly on the surfaces of Li-rich particles, could suppress the side reaction between the electrode and electrolyte, enhancing the cycling stability. Moreover, the presence of the spinel phase supplied fast three-dimensional Li^+ diffusion channels, thus leading to superior rate capacity. Meanwhile, it shortened the voltage plateau at approximately 4.5 V and increased the plateau length by approximately 2.8 V during the initial charge–discharge process, resulting in an ultrahigh initial Coulombic efficiency, which reached nearly 100%.

Carbon materials are ideal electronic conductors, which could offset the drawback of low electronic conductivity in LLOs if carbon and Li-rich cathode materials are combined[93-95]. However, it is difficult to coat carbon on the surfaces of LLOs because carbon always shows a tendency to reduce the transition metal ions at high-temperature calcination, which has a negative effect on the crystal structure of materials[96, 97]. Xia et al.[98] fabricated a layered @ spinel @ carbon hetero-structure for Li-rich cathode materials by a novel method called bio-inspired coating. This method employs a biomolecule dopamine as the carbon source, which is deposited on the surfaces of LLOs by self-polymerizing in an alkaline solution to form a uniform polydopamine layer. The subsequent carbonization process triggers the phase transition from layer to spinel, resulting in a multi-layer hetero-structure material with facile electron transport pathways and 3D Li^+ diffusion channels. This novel material has an extremely high discharge capacity of 334.5 mA h g^{-1} and excellent rate stability.

6. OLIVINE-LAYERED HETEROGENEOUS STRUCTURE

In addition to Mn-based spinel cathode materials, olivine $LiFePO_4$ as a cathode material has great advantages with satisfactory structural stability and desirable electron/ion transfer pathways.

Integrating $LiFePO_4$ and Li-rich layered oxides will result in excellent electronic and ionic conductivity, effectively improving the electrochemical performance. For example, Zheng et al.[99] coated electrochemically active nano-$LiFePO_4$ on the surfaces of LLOs by a facile sol-gel method. They proposed that Fe would occupy the Li site to prevent transition metal migration after the surface treatment of citric acid on the LLOs at high-temperature calcinations. PO_4^{3-} would occupy the cubic closely packed oxygen sites to change the local environment of the layer structure and stabilize the transition metal, which immensely suppressed the voltage fade (Fig. 12b-d). In addition, $LiFePO_4$ as the electronic and Li^+ conductors offered a fast charge transport pathway on the surfaces of the LLOs, presenting an outstanding discharge capacity of 282.8 mAh g^{-1} at 0.1 C and a superior cycling property (Fig. 12a). In a similar way, Martha et al.[100] used solid electrolyte LiPON to coat LLOs by an RF-magnetron sputtering method. This nanometre-thick Li^+ conductor endowed the LLO materials with excellent rate stability and cycle performance.

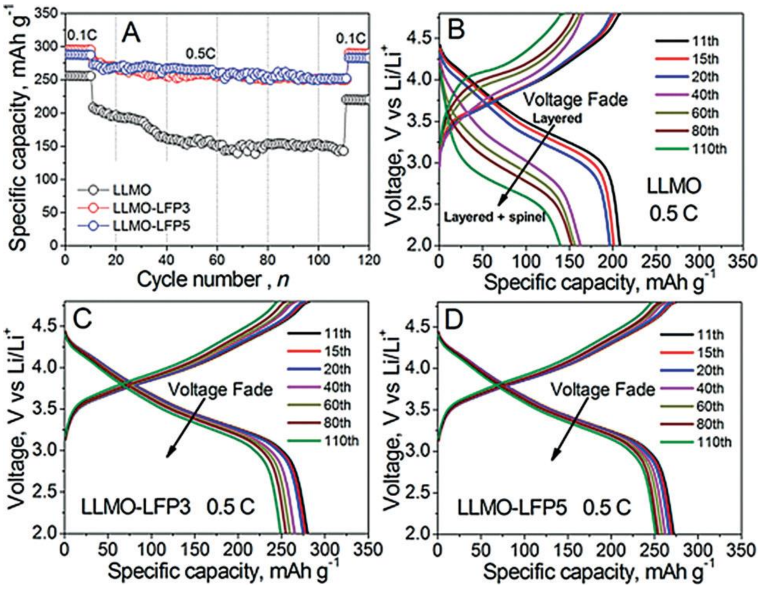

Figure 12. (a) Cycling performance and (b-d) charge-discharge curves of batteries based on LLMO, LLMO-LFP3, and LLMO-LFP5 cathode materials at 0.5 C between 2.0 and 4.8 V (vs. Li/Li+) at room temperature. Reprinted with permission from Wiley VCH[99].

7. TUNING THE LATTICE STRUCTURE

Since the O 2p band in polyanions has lower energy compared to the lattice O of Li-rich cathode materials, polyanions could improve the structural stability if they partially substitute the lattice O of Li-rich cathode materials. Additionally, the central element in polyanions would affect the bond length of the transition metal and oxygen, regulating the electronic structure. Li et al.[36] reported a novel strategy to decrease the M-O covalency (Fig. 13) and lower the O 2p band top by incorporating the $(BO_4)^{n-}$-like polyanion or its derivatives to substitute the lattice O, which could stabilize the oxygen closely packed structure, improving the electrochemical performance. This modified material exhibited a superior initial reversible capacity of 319 mAh g^{-1} and an excellent capacity retention of 94% after 80 cycles and 89% after 300 cycles of charge/discharge.

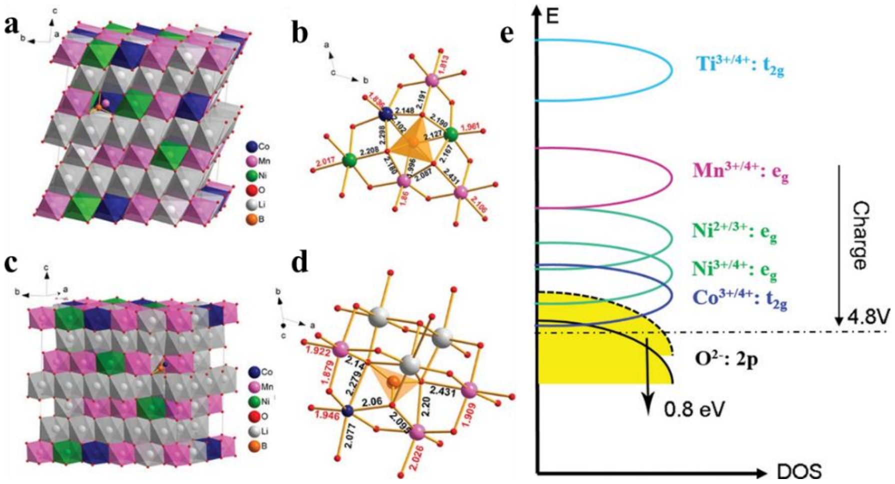

Figure 13. DFT-simulated structure of B_x-LRM. Schematic diagram of the optimized crystal structure of B_x-LRM with (a) BO_4 and (c) BO_3; (b) and (d) show their local structures around the polyanions, respectively. (e) Schematic diagram of the charge compensation mechanism before and after boracic polyanion substitution. Reprinted with permission from Wiley VCH[36].

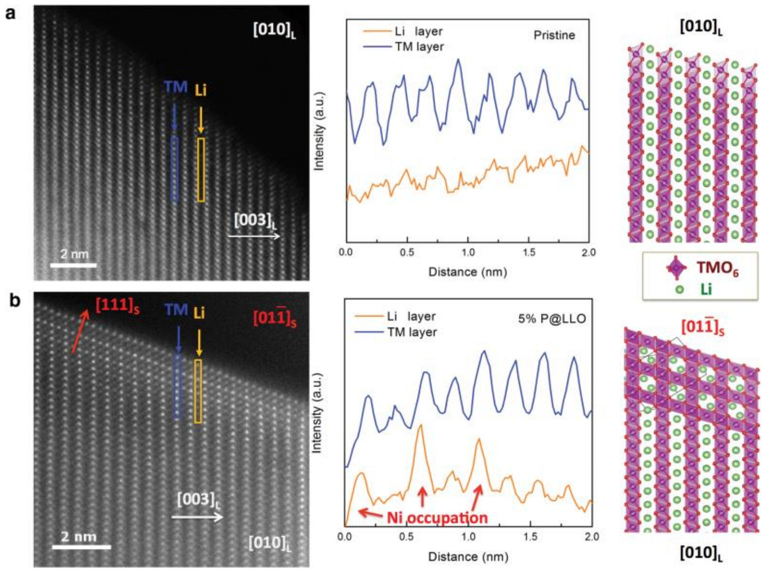

Figure 14. Comparison of HAADF-STEM images, corresponding line profiles and crystallographic model of as-prepared LLOs with and without PO_4^{3-} doping. (a) Pristine material along the [010] zone axis. (b) 5% P@LLO material with a spinel surface and the layered bulk along the [011] and [010] zone axes, respectively. Reprinted with permission from Wiley VCH[37].

In addition to $(BO_4)^{n-}$, other polyanions such as PO_4^{3-} and SiO_4^{4-} were also explored to modify the Li-rich cathode materials [37, 101]. For example, Zhao et al.[37] incorporated gradient polyanion PO_4^{3-} into Li-rich cathode materials by an ordinary co-precipitation method. They discovered a spinel-like layer of approximately 2 nm on the surface, which stabilized the closely packed oxygen structure, facilitated Li^+ transfer, and prevented the side reaction between the electrode material and electrolyte during the cycling process.

The presence of PO_4^{3-} along the (010) zone axis was verified by high angle annular dark field-scanning transmission electron microscopy (HAADF-STEM) (Fig. 14) and XPS. It was also found that P occupied tetrahedral interstitial sites, inducing changes in the M-O and Li-O lattices. At the same time, gradient PO_4^{3-} would cause the partial replacement of Mn by Ni or P on the surface of the Li-rich cathode material, reducing the irreversible capacity loss during the initial Li insertion/reinsertion process, leading to a high initial Coulombic efficiency of 86% compared to 72% of pristine Li-rich cathode materials.

8. CONCLUSIONS

In this review, we briefly introduce the structure and charge–discharge mechanism of LLOs. Some efforts and results of designing new Li-rich cathode materials to overcome technical challenges, such as a low initial Coulombic efficiency, poor rate capacity and cycling stability, are summarized. These efforts have yielded great progress in improving the electrochemical performance of Li-rich materials, such as layered-spinel composite materials and 3D spheres self-assembled by nanoplates. However, the detailed mechanism is not clear for these strategies, and the electrochemical performance of Li-rich materials can be further increased. Based on recent progress, we believe that future research directions for Li-rich cathode materials should focus on the following aspects: 1) precise and facile control of the composition and structure of heterogeneous Li-rich cathode materials such as layered-spinel oxides and clarification of their mechanism will be helpful in developing novel structures with high electrochemical performance and structural stability; 2) because LLOs could show a high discharge capacity in the voltage window of 2.0-4.8 V because of their unique charge–discharge mechanism, which, however, leads to severe electrolyte decomposition, the development of LLOs with a lower operating voltage range and superior electrochemical performance will be a significant contribution to Li-rich cathode materials; and 3) exposing preferential crystal planes or forming 3D porous structures to offer unobstructed Li^+ transfer pathways and improve the electrochemical performance. However, these materials are usually inferior from the point of view of commercial application in terms of their tap density and surface area. Hence, it will be helpful to increase the tap density and lower surface area of these materials for practical applications.

ACKNOWLEDGEMENTS
This work was financially supported by the Science and Technology Program of the State Grid Corporation of China (Program Title: Development of low cost and high safety lithium ion battery based on manganese series).

References

1. M.M. Thackeray, C. Wolverton, E.D. Isaacs, *Enger. Environ. Sci.,* 5 (2012) 7854.
2. M.S. Whittingham, *Chem. Rev.,* 104 (2004) 4271.
3. J.M. Tarascon and M. Armand tarascon, *Nature*, 414 (2001) 359.
4. L. Gu, C.B. Zhu, H. Li, Y. Yu, C.L. Li, S. Tsukimoto, J. Maier, Y. Ikuhara, *J. Am. Chem. Soc.,* 133 (2011) 4661.
5. B Dunn, H. Kamath and J.M. Tarascon, *Science,* 334 (2011) 928.
6. M.M. Thackeray, S.H. Kang, C.S. Johnson, J.T. Vaughey, R. Benedek, S.A. Hackney, *J. Mat. Chem.,* 17 (2007) 3112.
7. J. Wang, X. He, E. Paillard, N. Laszczynski, J. Li, S. Passerini, *Adv. Energy Mater.,* 6 (2016) 1600906.
8. S. Hy, F. Felix, J. Rick, W.N. Su, B.J. Hwang, *J. Am. Chem. Soc.,* 136 (2014) 999.
9. H.J. Yu and H.S. Zhou, *J. Phys. Chem. Lett.,* 4 (2013) 1268.
10. N. Yabuuchi, K. Yoshii, S.T. Myung, I. Nakai, S. Komaba, *J. Am. Chem. Soc.,* 133 (2011) 4404.
11. Y.S. Hong, Y.J. Park, K.S. Ryu, S.H. Chang, M.G. Kim, *J. Mater. Chem.,* 14 (2004) 1424.
12. F. Zhou, X.M. Zhao, A. van Bommel, X. Xia, J.R. Dahn, *J. Electrochem. Soc.,* 158 (2011) A187.
13. A.R. Armstrong, M. Holzapfel, P. Novak, C.S. Johnson, S.H. Kang, M.M. Thackeray, P.G. Bruce, *J. Am. Chem. Soc.,* 128 (2006) 8694.
14. C.S. Johnson, J.S. Kim, C. Lefief, N. Li, J.T. Vaughey, M.M. Thackeray, *Electrochem. Commun.,* 6 (2004) 1085.
15. C.P. Grey, W.S. Yoon, J. Reed, G. Ceder, *Electrochem. Solid ST.,* 7 (2004) A290.
16. K. Kang and G. Ceder, *Phys. Rev. B.,* 74 (2006).
17. Z.H. Lu, L.Y. Beaulieu, R.A. Donaberger, C.L. Thomas, J.R. Dahn, *J. Electrochem. Soc.,* 149 (2002) A778.
18. H. Kim, M.G. Kim, H.Y. Jeong, H. Nam, J. Cho, *Nano Lett.,* 15 (2015) 2111.
19. S. Hy, J.H. Cheng, J.Y. Liu, C.J. Pan, J. Rick, J.F. Lee, J.M. Chen, B.J. Hwang, *Chem. Mater.,* 26 (2014) 6919.
20. Y. Xie, M. Saubanère, and M.L. Doublet, *Energy Environ. Sci.,* 10 (2017) 266.
21. M. Sathiya, A.M. Abakumov, D Foix, G. Rousse, K. Ramesha, M. Saubanere, M.L. Doublet, H. Vezin, C.P. Laisa, A.S. Prakash, D. Gonbeau, G. VanTendeloo, J.M. Tarascon, *Nat. Mater.,* 14 (2015) 230.
22. B. Li and D.G. Xia, *Adv. Mater.,* 29 (2017).
23. P.E. Pearce, A.J. Perez, G. Rousse, M. Saubanere, D. Batuk, D. E. McCalla, A.M. Abakumov, G. Van Tendeloo, M.L. Doublet, J.M. Tarascon, *Nat. Mater.,* 16 (2017) 580.
24. D. Luo, S.H. Fang, Q.H. Tian, L. Qu, L. Yang, S.I. Hirano, *Nano Energy,* 21 (2016) 198.
25. M.N. Ates, Q.Y. Jia, A. Shah, A. Busnaina, S. Mukerjee, K.M. Abraham, *J. Electrochem. Soc.,* 161 (2013) A290.
26. E. Lee, J.S. Park, T.P. Wu, C.J. Sun, H. Kim, P.C. Stair, J. Lu, D.H. Zhou, C.S. Johnson, *J. Mater. Chem. A.,* 3 (2015) 9915.
27. Y.Q. Wang, Z.Z. Yang, Y.M. Qian, L. Gu, H.S. Zhou, *Adv. Mater.*, 27 (2015) 3915.
28. N. Li, R. An, Y.F. Su, F. Wu, L.Y. Bao, L. Chen, Y. Zheng, *J. Mater. Chem. A.*, 1 (2013) 9760-9767.
29. Z. Zheng, X.D. Guo, Y.J. Zhong, W.B. Hua, C.H. Shen, S.L. Chou, X.S. Yang, *Electrochim. Acta,* 188 (2016) 336.
30. Q. Li, G.S. Li, C.C. Fu, D. Luo, J.M. Fan, L.P. Li, *ACS. Appl. Mater. Interfaces,* 6 (2014) 10330.
31. R.P. Qing, J.L. Shi, D.D. Xiao, X.D Zhang, Y.X. Yin, Y.B. Zhai, L. Gu, Y.G. Guo, *Adv. Energy Mater.,* 6 (2016) 1501914.
32. J.K. Zhao, Z.X. Wang, H.J. Guo, X.H. Li, Z.J. He, T. Li, *Ceram. Int.,* 41 (2015) 11396.
33. H. Xu, Deng. S and Chen. G, *J. Mater. Chem. A.,* 2 (2014) 15015.

34. T.F. Yi, Y.M. Li, S.Y. Yang, Y.R. Zhu, Y Xie, *ACS. Appl. Mater. Interfaces,* 8 (2016) 32349.
35. H.Z. Zhang, Q.Q. Qiao, G.R. Li, X.P. Gao, *J. Mater. Chem. A.,* 2(2014):7454-7460.
36. B. Li, H.J. Yan, J. Ma, P.R. Yu, D.G. Xia, W.F. Huang, W.S. Chu, Z.Y. Wu, *Adv. Funct. Mater.,* 24 (2014) 5112.
37. Y. Zhao, J.T. Liu, S.B. Wang, R. Ji, Q.B. Xia, Z.P. Ding, W.F. Wei, Y. Liu, P. Wang, D.G. Ivey, *Adv. Funct. Mater.,* 26 (2016) 4760.
38. J Liu, S B Wang, Z.P. Ding, R.Q. Zhou, Q.B. Xia, J.F. Zhang, L.B. Chen, W.F. Wei, P. Wang, (2016) *ACS. Appl. Mater. Interfaces,* 8 (2016) 18008.
39. J.Z. Kong, H.F. Zhai, X. Qian, M. Wang, Q.Z. Wang, A.D. Li, H. Li, F. Zhou, *J. Alloys Compounds,* 694 (2017) 848.
40. R.B. Yu, Y.B. Lin, and Z.G. Huang, *Electrochim. Acta,* 173 (2015) 515.
41. G.X. Fan, H.L. Li, S.P. Dai, C.X. Zhang, X.M. Guan, Z.R. Chang, B.Z. Liu, *Mater. Res. Bull.,* 57 (2014) 274.
42. S.J. Shi, J.P. Tu, Y.Y. Tang, X.Y. Liu, Y.Q. Zhang, X.L. Wang, C.D. Gu, *Electrochim. Acta,* 88 (2013) 671.
43. G. Kobayashi, Y. Irii, F. Matsumoto, A. Ito, Y. Ohsawa, S Yamamoto, Y.T. Cui, J.Y. Son, Y.C. Sato, *J. Power Sources,* 303 (2016) 250.
44. H. Liu, H.D. Liu, D.N. Qian, M.G. Verde, M.H. Zhang, L. Baggetto, K. An, Y. Chen, K.J. Carroll, D. Lau, M.F. Chi, G.M. Veith, Y.S. Meng, *ACS. Appl. Mater. Interfaces,* 7 (2015) 19189.
45. M. Xu, Z.Y. Chen, L.J. Li, H.L. Zhu, Q.F. Zhao, L. Xu, N.F. Peng, L. Gong, *J. Power Sources,* 281 (2015) 444.
46. X.F. Zhang, I. Belharouak, L. Li, Y. Lei, J.W. Elam, A.M. Nie, X.Q. Chen, R.S. Yassar, R.L. Axelbaum, *Adv. Energy Mater.*, 3 (2013) 1299.
47. X.M. Zhu, Y.X. Wang, K.H. Shang, W. He, X.P Ai, H.X. Yang, Y.L. Cao, *J. Mater. Chem. A.,* 3 (2015) 17113.
48. S. Sun, *ChemSusChem,* 8 (2015) 2544.
49. J.M. Zheng, M. Gu, J. Xiao, B.J. Polzin, P.F. Yan, X.L. Chen, C.M. Wang, J.G. Zhang, *Chem. Mater.,* 26 (2014) 6320.
50. K.J. Rosina, M. Jiang, D.L. Zeng, E. Salager, A.S. Best, C.P. Grey, *J. Mater. Chem.,* 22 (2012) 20602.
51. X.Y. Liu, T. Huang, and A.S. Yu, *Electrochim. Acta,* 163 (2015) 82.
52. S.K. Chong, Y.Z. Chen, W.W. Yan, S.W. Guo, Q. Tan, Y.F. Wu, T. Jiang, Y.N. Liu, *J. Power Sources,* 332 (2016) 230.
53. T.L. Zhao, L. Li, R.J. Chen, H.M. Wu, X.X. Zhang, S. Chen, M. Xie, F. Wu, J. Lu, K. Amine, *Nano Energy,* 15 (2015) 164.
54. F. Wu, X.X. Zhang, T.L. Zhao, L. Li, M. Xie, R.J. Chen, *ACS. Appl. Mater. Interfaces,* 7 (2015) 3773.
55. D.R. Chen, F. Zheng, L. Li, M. Chen, X.X. Zhong, W.S. Li, L. Lu, *J. Power Sources,* 341 (2017).
56. H. Liu, C. Chen, C.Y. Du, X.S. He, G.P. Yin, B. Song, P.J. Zuo, X.Q. Cheng, Y.L. Ma, Y.Z. Gao, *J. Mater. Chem. A.,* 3 (2015) 2634.
57. F.X. Wang, S.Y. Xiao, M.X. Li, X.W. Wang, Y.S. Zhu, Y.P. Wu, A. Shirakawa, J. Peng, *J. Power Sources,* 287 (2015) 416.
58. Z.Y. Wang, E.Z. Liu, C.N. He, C.S. Shi, J.J. Li, N.Q. Zhao, *J. Power Sources,* 236 (2013) 25.
59. Q.Q. Qiao, H.Z. Zhang, G.R. Li, S.H. Ye, C.W. Wang, X.P. Gao, *J. Mater. Chem. A.,* 1 (2013) 5262.
60. Q.R. Xue, J.L. Li, G.F. Xu, H.W. Zhou, X.D. Wang, F.Y. Kang, *J. Mater. Chem. A.,* 2 (2014) 18613.
61. P. Oh, M. Ko, S. Myeong, Y. Kim, J. Cho, *Adv. Energy Mater.,* 4 (2014) 1400631.
62. W. Liu, P. Oh, X. Liu, S. Myeong, W. Cho, J. Cho, *Adv. Energy Mater.,* 5(2015) 1500274.
63. D.H. Park, S.T. Lim, S.J. Hwang, C.S. Yoon, Y.K. Sun, J.H. Choy, *Adv. Mater.,* 17 (2005) 2834.

64. N. Balke, S. Jesse, A.N. Morozovska, E. Eliseev, D.W. Chung, Y. Kim, L. Adamczyk, R.E. Garcia, N. Dudney, S.V. Kalinin, *Nat. Nanotechnol.,* 5 (2010) 749.
65. N. Igawa, T. Taguchi, H. Fukazawa, H. Yamauchi, W. Utsumi, *J. Am. Ceram. Soc.,* 93 (2010) 2144.
66. F. Fu, G.L. Xu, Q. Wang, Y.P. Deng, X. Li, J.T. Li, L. Huang, S.G. Sun, *J. Mater. Chem. A.,* 1 (2013) 3860.
67. J. Li, R. Yao and C. Cao, *ACS. Appl. Mater. Interfaces,* 6 (2014) 5075.
68. H.L. Chen and C.P. Grey, *Adv. Mater.,* 20 (2008) 2206.
69. G.Z. Wei, X. Lu, F.S. Ke, L. Huang, J.T. Li, Z.X. Wang, Z.Y. Zhou, S.G. Sun, *Adv. Mater.,* 22 (2010) 4364.
70. L. Chen, Y.F. Su, S. Chen, N. Li, L.Y. Bao, W.K. Li, Z. Wang, M. Wang, F. Wu, *Adv. Mater.,* 26 (2014) 6756.
71. J.L. Liu, L. Chen, M.Y. Hou, F. Wang, R.C. Che, Y.Y. Xia, (2012) *J. Mater. Chem.,* 22 (2012) 25380.
72. M. Xu, L.F. Fei, W.B. Zhang, T. Li, W. Lu, N. Zhang, Y.Q. Lai, Z. Zhang, J. Fang, K. Zhang, J. Li, H.T. Huang, *Nano Lett.,* 17 (2017) 1670.
73. R. Huang, Y.H. Ikuhara, T. Mizoguchi, S.D. Findlay, A. Kuwabara, C.A.J. Fisher, H. Moriwake, H. Oki, T. Hirayama, Y. Ikuhara, *Angew. Chem. Int. Ed. Engl.*, 50 (2011) 3053.
74. P.V. Sushko, K.M. Rosso, J.G. Zhang, J. Liu, M.L. Sushko, *Adv. Funct. Mater.,* 23 (2013) 5530.
75. B. Qiu, M.H. Zhang, L.J. Wu, J. Wang, Y.G. Xia, D.N. Qian, H.D. Liu, S. Hy, Y. Chen, K. An, Y.M. Zhu, Z.P. Liu, Y.S. Meng, *Nat. Commun.,* 7 (2016) 12108.
76. C. Chen, T.F. Geng, C.Y. Du, P.J. Zuo, X.Q. Cheng, Y.L. Ma, G.P. Yin, *J. Power Sources,* 331 (2016) 91.
77. M. Xu, L.F. Fei, W. Lu, Z.Y. Chen, T. Li, Y. Liu, G.Y. Gao, Y.Q. Lai, Z.A. Zhang, P. Wang, H.T. Huang, *Nano Energy,* 35 (2017) 271.
78. M.M. Thackeray, C.S. Johnson, J.T. Vaughey, N. Li, S.A. Hackney, *J. Mater. Chem.,* 15 (2005) 2257.
79. J.Y. Cao, J. Xie, G.S. Cao, T.J. Zhu, X.B. Zhao, S.C. Zhang, *Electrochim. Acta,* 111 (2013) 447.
80. S. Ivanova, E. Zhecheva, D. Nihtianova, M. Mladenov, R. Stoyanova, *J. Alloy. Compd.,* 561 (2013) 252.
81. A. Bhaskar, W. Gruner, D. Mikhailova, H. Ehrenberg, *RSC Advances,* 3 (2013) 5909.
82. J. Xiao, X.L. Chen, P.V. Sushko, M.L. Sushko, L. Kovarik, J.J.Feng, Z.Q. Deng, J.M. Zheng, G.L. Graff, Z.M. Nie, D.W. Choi, J. Liu, J.G. Zhang, M.S. Whittingham, *Adv. Mater.,* 24 (2012) 2109.
83. J.R. Croy, S.H. Kang, M. Balasubramanian, M.M. Thackeray, *Electrochem. Commun.,* 13 (2011) 1063.
84. E.S. Lee, A. Huq, H.Y. Chang, A. Manthiram, *Chem. Mater.,* 24 (2012) 600.
85. D. Kim, G. Sandi, J.R. Croy, K.G. Gallagher, S.H. Kang, E. Lee, M.D. Slater, C.S. Johnson, M.M. Thackeray, *J. Electrochem. Soc.,* 160 (2012) A31.
86. A. Bhaskar, S. Krueger, V. Siozios, J. Li, S. Nowak, M. Winter, *Adv. Energy Mater.,* 5 (2015) 1401156.
87. Y.F. Chen, K. Xie, C.M. Zheng, Z.Y. Ma, Z.X. Chen, *ACS. Appl. Mater. Interfaces,* 6 (2014) 16888.
88. E.S. Lee, A. Huq, and A. Manthiram, *J. Power Sources,* 240 (2013) 193.
89. J. Song, D.W. Shin, Y.H. Lu, C.D. Amos, A. Manthiram, J.B. Goodenough, *Chem. Mater.,* 24 (2012) 3101.
90. D. Luo, G.S. Li, C.C. Fu, J. Zheng, J.M. Fan, Q. Li, L.P. Li, *Adv. Energy Mater.,* 4 (2014) 1400062.
91. Y. Pei, C.Y. Xu, Y.C. Xiao, Q. Chen, B. Huang, B. Li, S. Li, L. Zhen, G.Z. Cao, *Adv. Funct. Mater.,* 27 (2017):1604349.
92. H. Liu, C.Y. Du, G.P. Yin, B. Song, P.J. Zuo, X.Q. Cheng, Y.L. Maa, Y.Z. Gao, *J. Mater. Chem.*

A., 2 (2014) 15640.
93. B. Song, M.O. Lai, Z.W. Liu, H.W. Liu, L. Lu, *J. Mater. Chem. A.,* 1 (2013) 9954.
94. C.H. Jiang, Z.L. Tang, S.Q. Deng, Y. Hong, S.T. Wang, Z.T. Zhang, *RSC. Adv.,* 7 (2017) 3746.
95. B. Song, H.W. Liu, Z.W. Liu, P.F. Xiao, M.O. Lai, L. Lu, *Sci. Rep.,* 3 (2013) 3094.
96. J.B. Goodenough and Y. Kim, *Chem. Mater.,* 22 (2010) 587.
97. X. He, J. Wang, R. Wang, B. Qiu, H. Frielinghaus, P. Niehoff, H.D. Liu, M.C. Stan, E. Paillard, M. Winter, J. Li, *J. Mater. Chem. A.,* 4 (2016) 7230.
98. Q.B. Xia, X.F. Zhao, M.Q. Xu, Z.P. Ding, J.T. Liu, L.B. Chen, D.G. Ivey, W.F. Wei, *J. Mater. Chem. A.,* 3 (2015) 3995
99. F.H. Zheng, C.H. Yang, X.H. Xiong, J.W. Xiong, R.Z. Hu, Y. Chen, M.L. Liu, *Angew. Chem. Int. Ed. Engl.,* 54 (2015) 13058.
100. S.K. Martha, J. Nanda, Y. Kim, R.R. Unocic, S. Pannala, N.J. Dudney, *J. Mater. Chem. A.,* 1(2013) 5587.
101. J. Ma, H.J. Yan, B. Li, Z.H. Xia, W.F. Huang, L. An, D.G. Xia, *J. Phys. Chem. C,* 120 (2016) 13421.